Manipulation and Mechanical Deformation of Leukemia Cells by High-Frequency Ultrasound Single Beam

Yushun Zeng, *Member, IEEE*, Jia Hao, Junhang Zhang, *Member, IEEE*, Laiming Jiang, Sangyeon Youn, Gengxi Lu, *Member, IEEE*, Dongliang Yan, Haochen Kang, *Graduate Student Member, IEEE*, Yizhe Sun, *Member, IEEE*, K. Kirk Shung, *Life Fellow, IEEE*, Keyue Shen, and Qifa Zhou, *Fellow, IEEE*

***Abstract*— Ultrasound single-beam acoustic tweezer system has attracted increasing attention in the field of biomechanics. Cell biomechanics play a pivotal role in leukemia cell functions. To better understand and compare the cell mechanics of the leukemia cells, herein, we fabricated an acoustic tweezer system in-house connected with a 50-MHz high-frequency cylinder ultrasound transducer. Selected leukemia cells (Jurkat, K562, and MV-411 cells) were cultured, trapped, and manipulated by high-frequency ultrasound single beam, which was transmitted from the ultrasound transducer without contacting any cells. The relative deformability of each leukemia cell was measured, characterized, and compared, and the leukemia cell (Jurkat cell) gaining the highest deformability was highlighted. Our results demonstrate that the high-frequency ultrasound single beam can be utilized to manipulate and characterize leukemia cells, which can be applied to study potential mechanisms in the immune system and cell biomechanics in other cell types.**

***Index Terms*— Acoustic tweezer, high-frequency ultrasound, leukemia cells, ultrasound transducer.**

I. Introduction

THE mechanical properties of the cell are of great significance to cellular functions. In normal cells, cellular biomechanics have been associated with cell differentiation, blockade of viral infection, and metabolism [1]–[3]. On the other hand, cancer cells have higher deformability than normal cells, which allows them to squeeze through extracellular matrix (ECM) and endothelial cell–cell junctions to reach a distant site during metastasis [4], [5]. As a result, the mechanical properties, such as stiffness and plasticity, of a cancer cell can serve as a biomarker for the metastatic potential and detection of metastatic cells in various cancers [6]–[8]. Hematologic malignancies or leukemia constitute an important class of cancer diseases [9]–[16]. Particularly, leukemia has various mechanisms, such as acute T lymphocyte leukemia (ALL), acute myeloid leukemia (AML), and chronic myeloid leukemia (CML), and it is critical to provide a treatment suitable for each mechanism [17]–[20]. To provide faster diagnosis and efficient cancer treatment, characterization studies of various leukemia cells are in progress. Changes in cell mechanical properties of leukemic cells can have profound effects on their ability to circulate in the vasculature, e.g., increased stiffness impairs the trafficking of cells through tiny capillaries [21], [22]. A study using optical tweezers demonstrated that regular and leukemic hematopoietic cell populations with distinct primitiveness have differential deformability [9]. Recently, higher cellular rigidity has been revealed as a crucial factor in maintaining normal hematopoietic stem cells (HSCs) and their regenerative ability in the bone marrow, while increasing the deformability of leukemic cells through genetic manipulation significantly accelerated the disease progression [23], [24]. A better understanding of the biophysical properties of leukemic cells, such as deformability, is thus crucial for an improved understanding of the disease.

Many useful biophysical tools have been developed and utilized to quantify cell mechanics, including atomic force microscopy (AFM), optical tweezers, and magnetic tweezers [25]–[35]. However, these methods apply poorly to the biomechanical quantification of leukemic cells. Normal and malignant hematopoietic cells at their resting state are nonadhesive, which poses a significant challenge for AFM as they often slip from the cantilever tip under mechanical loads [22]. In the studies of optical tweezers, the laser will cause high temperature that can damage the biological specimens [36]–[38]. Although magnetic tweezers have a

Manuscript received April 17, 2022; accepted April 21, 2022. Date of publication April 25, 2022; date of current version May 26, 2022. The work of Keyue Shen was supported by the National Institute of Health (NIH) under Grant R01CA220012. The work of Qifa Zhou was supported by the NIH under Grant R01HL125084 and Grant R01NS111039. *(Yushun Zeng, Jia Hao, and Junhang Zhang contributed equally to this work.) (Corresponding authors: Keyue Shen; Qifa Zhou.)*

Yushun Zeng, Junhang Zhang, Laiming Jiang, Sangyeon Youn, Gengxi Lu, Dongliang Yan, Haochen Kang, Yizhe Sun, and Qifa Zhou are with the Department of Biomedical Engineering, Viterbi School of Engineering, University of Southern California, Los Angeles, CA 90089 USA, and also with the Keck School of Medicine, Roski Eye Institute, University of Southern California, Los Angeles, CA 90033 USA (e-mail: qifazhou@usc.edu).

Jia Hao and Keyue Shen are with the Department of Biomedical Engineering, Viterbi School of Engineering, University of Southern California, Los Angeles, CA 90089 USA, and also with the Norris Comprehensive Cancer Center, USC Stem Cell, University of Southern California, Los Angeles, CA 90033 USA (e-mail: keyue.shen@usc.edu).

K. Kirk Shung is with the Department of Biomedical Engineering, Viterbi School of Engineering, University of Southern California, Los Angeles, CA 90089 USA.

This article has supplementary downloadable material available at https://doi.org/10.1109/TUFFC.2022.3170074, provided by the authors.

Digital Object Identifier 10.1109/TUFFC.2022.3170074

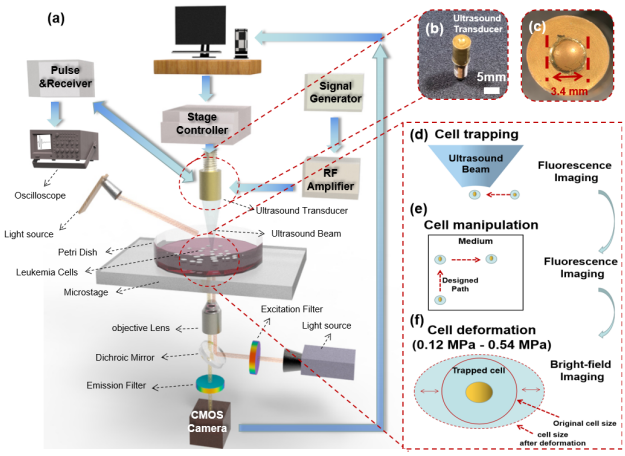

Fig. 1. (a) Schematic of acoustic tweezer setup developed in-house for cell experiment. (b) Optical image of fabricated 50-MHz LNO ultrasound transducer. (c) Top view of the fabricated LNO ultrasound transducer. Process of (d) cell trapping, (e) cell manipulation, and (f) cell deformation.

promising capability to achieve highly accurate forces to be transduced to molecules to investigate mechanotransduction at the cellular level, it relies on the attachment of cells and molecules to various magnetic beads to be manipulated by magnetic field [26], [39], [40]. Hence, these drawbacks hinder the direct quantification of cell mechanics. Recently, several noncontact acoustic tweezers have been developed to investigate the mechanical properties of cells, as they can cause less cell damage and generate a higher force to trap cells [41]–[50]. In addition to the method of measuring the mechanical properties of cells using acoustic trapping, studies have been conducted to measure the various biochemical properties of the cells for the fundamental treatment of cancer. Youn *et al.* [51], [52] studied research to characterize the metastasis of cancer cells by analyzing the phenomenon that the acoustic pressure generated during cell trapping induces mechanical stress in the membrane, which causes calcium ions to flow into the cell. In addition, the deep learning-based fluorescent cell analysis algorithm can automatically recognize the trapped cell among the suspended cells and analyze the intensity variation of the cell during the trapping. The automatic segmentation, recognition of trapped cells, and the calcium ion analysis algorithm can greatly shorten the time for analyzing the cell properties and increase the reliability of the cancer cell metastasis discrimination system through more objective evaluation.

However, many of these tools require polymeric microbeads or carbon nanotubes to be attached to the membrane of target cells, and since calcium ion fluorescence imaging analyzes mechanotransduction rather than directly analyzing the mechanical properties of cells, it not only requires fluorescence dye but is also affected by the surrounding environment and state of cells. Additionally, the current acoustic tweezers with low frequency are also hard to manipulate or shift cells. Moreover, there are few investigations on the manipulation of various leukemia cells. These inspired us to develop a high-frequency acoustic tweezer technique for manipulating cells in a suspended medium without contacting target cells.

Herein, we developed a 50-MHz high-frequency acoustic tweezer system for cell manipulation and trapping without contacting targeted cells (Fig. 1), and we evaluated and quantitatively compared the relative deformability of three different leukemia cell lines, Jurkat, MV-411, and K-562, as models for ALL, AML, and CML, respectively. These cells can be successfully trapped and manipulated by our developed acoustic tweezer, and the Jurkat cell has shown higher relative deformability as 0.248 under acoustic peak pressure of 0.54 MPa. The results illustrate the comparative measurements of relative deformability, which will facilitate understanding the pathophysiologic characteristics of different hematopoietic malignancies. Furthermore, the significant feasibility of the high-frequency ultrasound single beam to measure the cell mechanics also shows more potential in applying high-frequency acoustic tweezer systems in the early diagnosis of leukemia and investigating various cell functions and mechanisms.

II. Materials and Methods

A. Ultrasound Transducer Fabrication for Acoustic Tweezer

A 50-MHz lithium niobate (LNO) ultrasound transducer was simulated and designed by a Krimboltz, Leedom, and Mattaei (KLM) transducer equivalent circuit model with PiezoCAD (Sonic Concepts Inc., Bothell, WA, USA). The purchased LNO material (Boston Piezo-Optics, Bellingham, MA, USA) was first lapped to the designed thickness (60 μm) and polished. Afterward, Au/Cr electrode was sputtered on both sides of the LNO by Sputter Coater (NSC-3000, Nano-Master, Inc., Austin, TX, USA). The sputtered LNO was diced into 5.5 mm $\times$ 5.5 mm and then machined into circular disks with a diameter of 3.4 mm by a lathe. For electrical interconnection, a 1.5-mm conductive silver paste (E-Solder 3022, VonRoll Isola, Schenectady, NY, USA) was employed and added on LNO circular disk as the backing layer, and the backed stack was then assembled into a brass housing. A subminiature version A (SMA) connector was connected with the inserted backing layer by a conductive wire. Another Au/Cr electrode was sputtered across the front surface of the LNO disk and the brass housing to build a ground connection. The transducer with a focal distance of 3.4 mm and an f-number of 1 was achieved by mechanical pressing a steel ball with a diameter of 6.8 mm. Finally, 10-μm parylene C was coated on the focused transducer by the parylene coater (Specialty Coating Systems Inc., Indianapolis, IN, USA). In Fig. 1(b) and (c), the optical images of the fabricated transducer are shown, and the transducer has an aperture size of 3.4 mm in diameter. To investigate the performance of the needle transducer, in Fig. 2(a)–(d), the impedance-phase angle spectrum and pulse-echo waveform of the simulated and fabricated transducer are shown. Simulated results were designed and gained by PiezoCAD. The impedance-phase angle spectrum of the transducer was characterized by the impedance analyzer (4294A, Agilent, Santa Clara, CA, USA), determining the resonance frequency (f_r) and antiresonance frequency (f_a) as 55 and 62 MHz separately. The impedance was located as 38–63 Ω from f_r to f_a. The generated

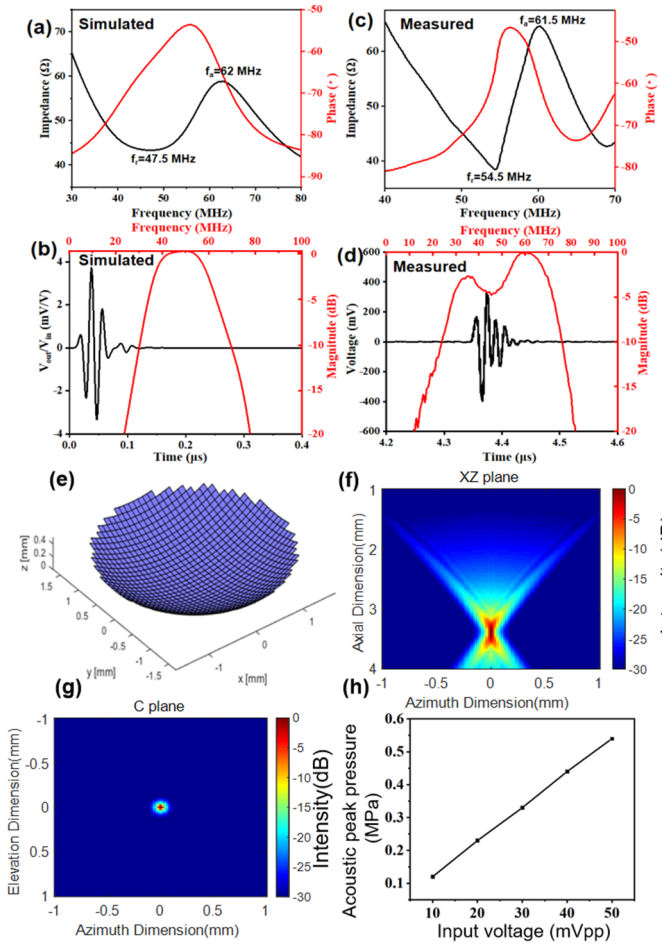

Fig. 2. (a) and (b) PiezoCAD simulated electrical impedance magnitude, phase, and pulse-echo waveform of the fabricated LNO ultrasound transducer. (c) and (d) Measured electrical impedance magnitude, phase, and pulse-echo waveform of the fabricated LNO ultrasound transducer. (e) Aperture simulation of fabricated LNO ultrasound transducer in field II. (f) and (g) Simulated emitting field in the *XZ* plane and *XY* plane in field II. (h) Tested acoustic peak pressure under different input voltages.

pulse-echo waveform [Fig. 2(d)] was measured as 0.8 V_{pp} by a self-developed pulse-echo system with pulser-and-receiver (Panametrics 5900PR, Olympus NDT Inc., State College, PA, USA) at damping of 50 Ω, 1 μJ/pulse, and pulse repetition frequency (PRF) of 200 Hz. The received pulse-echo signal was then transformed as a frequency spectrum via fast Fourier transform (FFT), demonstrating the central frequency (f_c) and −6-dB fractional bandwidth (BW) as 50 MHz and 89%, respectively. In Fig. 2(e)–(g), the acoustic field of the transducer was simulated in field II [53], [54]. The *XZ* plane and *C* plane results presented the emitting field of the aperture at $y = 0$ and $z = 3.4$ mm separately, in which the x, y, and z represented azimuth direction, elevation direction, and axial direction, respectively. According to the simulation results, −6-dB beamwidth at the focal point is 48 μm. The acoustic pressure was measured by the hydrophone (HGL-0400, ONDA, Sunnyvale, CA, USA) in a water tank (frequency: 50 MHz, number of cycles: ten, and the PRF: 1 kHz). In Fig. 2(h), the increased trend of formed acoustic peak pressures under different input voltages (10–50 mV_{pp}) of the fabricated transducer is shown. The input voltages from 10 to 50 mV_{pp} with 50-dB gain have generated the acoustic peak pressures of 0.12–0.54 MPa, which are similar to the measured results in previous works [49], [50].

B. Acoustic Tweezer System Setup

The schematic of the applied acoustic tweezer system is shown in Fig. 1(a). An inverted microscope (IX71, Olympus America Inc., Center Valley, PA, USA) was mechanically connected with the ultrasound transducer. Mercury lamp house (U-RFL-T, Olympus America Inc., Center Valley, PA, USA) and microscope external power supply halogen lamp house (TH4-100, Olympus America Inc., Center Valley, PA, USA) were connected with the microscope to provide light sources. An *XYZ* positioner (SGSP 50, Sigma KOKI Company, Tokyo, Japan) with a stage controller (SHOT-204MS, Sigma KOKI Company, Tokyo, Japan) was used to control and move the transducer connected with the acoustic system. The microstage of the microscope from the developed acoustic tweezer system was assembled as a platform to hold the petri dish. The fabricated ultrasound transducer was first connected with the pulser-and-receiver and the oscilloscope to test the pulse-echo performance. The transducer was placed into the medium of the petri dish containing the characterized cells, and the location of the transducer was optimized near the focal zone to gain the highest pulse-echo performance before cell trapping and manipulating, which could help to determine that the tested sample was under or near the focal point with highest ultrasound beam intensity. Afterward, the signal generator (SG384, Stanford Research Systems, Sunnyvale, CA, USA) connected with an RF power amplifier (525LA, Electronics and Innovations, Rochester, NY, USA) was combined to drive the transducer. The input voltage from signal generator was range from 10 to 50 mV_{pp} with 50-dB gain since the ultrasound transducer can be worked safely under these inputs. Hence, a 50-MHz sinusoidal burst waveform with the peak-to-peak voltage of 0.01–0.05 V_{pp}, PRF of 1 kHz, period of 1 ms, and 1% duty factor were adjusted in the signal generator, and the amplifier gained 50 dB to amplify 316 times for input voltage from the generator to drive the transducer, which transmitted the acoustic peak pressure as 0.12–0.54 MPa. Moreover, a charge-coupled device (CCD) camera (ORCA-Flash2.8, Hamamatsu Photonics K.K., Hamamatsu, Japan) installed in the microscope and position tracking software program (Metamorph Advanced, Olympus Corporation, Tokyo, Japan) was applied to capture the imaging files of cells with an exposure time of 15 ms during the trapping, manipulating, and deformation test.

C. Cell Preparation

Jurkat cells were cultured in the American Type Culture Collection (ATCC)-formulated RPMI-1640 Medium (Cat. ATCC 30-2001, ATCC, Manassas, VA, USA), and K-562 and MV-411 cells were cultured in Iscove's Modified Dulbecco's Medium (Cat. ATCC 30-2005, ATCC, Manassas, VA, USA), all supplemented with 10% fetal bovine serum (FBS) (Cat. F2442, Sigma-Aldrich, St. Louis, MO, USA) and 1% 100-U/mL penicillin-streptomycin (Sigma-Aldrich, St. Louis, MO, USA). Cells were subcultured every 2–3 days

and kept in sterile incubation conditions (37 °C, 5% CO_2, and 90% humidity) according to ATCC protocols. Cells were seeded at a concentration of 0.1 million/mL and prepared by the state suspended in Dulbecco's phosphate buffered saline (DPBS, Gibco, Franklin, TN, USA) to illustrate the ability of acoustic trapping, manipulation, and cell deformation. To increase the recognition degree of trapped cells, the cells were labeled with Calcein AM (Cat. C1430, Thermo Fisher Scientific, Waltham, MA, USA). Calcein AM is a cell-permeant dye for most eukaryotic cells, and it emits green fluorescence light due to blue excitation (excitation: 488 nm and emission: 515 nm). The stock solution of 1-mg/mL Calcein AM in dimethyl sulfoxide (DMSO) was diluted into 1-μM working concentration with serum-free media (same as culture media for each cell line). Cells were incubated with Calcein AM working solution for 20 min at 37 °C, washed once by centrifugation at 200× g for 5 min, and resuspended in fresh culture media.

D. Microscopy, Image Analysis, and Statistics for Leukemia Cells

A Nikon Eclipse Ti-E inverted fluorescence microscope (Nikon, Tokyo, Japan) and a 10× 0.45 numerical aperture (NA) air objective were used for live-cell imaging, equipped with an Okolab incubation box (Okolab, Pozzuoli, Italy) controlling for temperature (37 °C) and CO_2 concentration (5%). Images were analyzed using ImageJ (Version 1.53k, U.S. National Institutes of Health, Bethesda, MD, USA). Ordinary one-way analysis of variance (ANOVA) and Tukey's multiple comparisons test were performed in comparison of cell area. Data distribution was assumed to be normal, but this was not formally tested.

E. Cell Characterization by High-Frequency Ultrasound Single Beam

To test the cell trapping, manipulation, and deformation, cultured leukemia cells of Jurkat cell, K562 cell, and MV-411 cell were suspended and added to a 65-mm-diameter petri dish filled with a corresponding full culture medium. Calcein AM was added to label the cells. The petri dish was placed on the microstage of the acoustic tweezer system. The cell trapping, manipulation, and deformation processes have been shown in Fig. 1(d)–(f). In previous work, after the transducer was driven, the cells near or in the focal point would be shifted into the center of the point, as there had the highest acoustic beam intensity, and then held by the ultrasound beam when the trapping started [Fig. 1(d)]. Then, the trapped cell could be moved and manipulated on the bottom of the petri dish by following the designed path [Fig. 1(e)], which was mainly dominated by gradient force [41], [55]–[57]. After the ultrasound beam was applied, fluorescence imaging was utilized to locate and record the trapping and manipulation of live cells. Subsequently, in Fig. 1(f), the bright-field imaging was adjusted in the cell deformation test to analyze the cell areas. Afterward, fluorescence imaging was applied again to characterize the cell viability before and after the deformation test. To investigate the manipulation of leukemia cells, the input of the signal generator for the transducer was adjusted and turned on at 30 mV_{pp} (0.33 MPa) when the position of the transducer was optimized and determined. The cells were on the bottom of the petri dish. The trapped cell could be moved when the transducer was laterally shifted by the stage controller. As the input voltages of the transducer increased, according to the converse piezoelectric effect, the acoustic pressure transmitted from the transducer was enhanced to increase the scattering force, which would deform and stretch the trapped cells in a transverse direction under the ultrasound beam [Fig. 1(f)] [55]–[57]. Hence, during the deformation test, the input voltages in the signal generator were adjusted from 10 to 50 mV_{pp} with 50-dB gain, transmitting the acoustic peak pressure from 0.12 to 0.54 MPa. Areas of the stretched cells under different acoustic pressure can be recorded by connected CCD in acoustic tweezer system and analyzed via a Java-based image process program.

F. Cell Viability Evaluation

Cell viability tests of each cell were implemented before cell trapping and after cell deformation to evaluate whether the transmitting single ultrasound beam would cause cell death. Cultured Cells were added with LIVE/DEAD Cell Imaging Kit (Catalog No. R37601, Invitrogen, Thermo Fisher Scientific, Waltham, MA, USA) according to the manufacturer's protocol. The LIVE/DEAD Cell Imaging Kit consists of two reagents. Calcein AM (in green, excitation: 488 nm and emission: 515 nm) stains the live cell, and BOBO-3 Iodide (in red, excitation: 570 nm and emission: 602 nm) stains the nuclei of the dead cells. Afterward, the fluorescence microscopy staining imaging of live and dead cells was recorded to calculate the cell viability. To prepare the cells for testing their viability, 1 mL of LIVE Green was transferred to the DEAD Red vial, including 1 μL of DEAD Red, and mixed to create a 2× working solution. An equal volume of 2× working solution was added to the prepared cells suspended in phosphate-buffered saline (PBS). After incubating for 15 min at room temperature, the cell viability test proceeded. To examine whether the applied ultrasound can damage cells when deformability is measured, we stimulated each cell line for 25 min, which exceeded the stimulation time in the experiment for measuring relative deformability. Finally, the viability of 12 cells in each cell line (Jurkat, K-562, and MV-411) was calculated.

III. Results

A. Noncontact Single Cell Manipulation

Under normal culture conditions, Jurkat, K562, and MV-411 cells show different cell areas [Fig. 3(a) and (b)]. The diameters of the three cells are less than the focal point of the fabricated transducer, which could imply better cell trapping and manipulation in the following test. CML cell line, K562, was characterized as having the highest cell area (77.2 ± 13.2 μm^2) compared to acute leukemia cell lines, Jurkat (61.0 ± 15.6 μm^2) and MV-411 (42.5 ± 8.45 μm^2).

The optimized distance between transducer and bottom of petri dish was close to the focal length of the transducer, which can make the transducer gain the highest pulse-echo

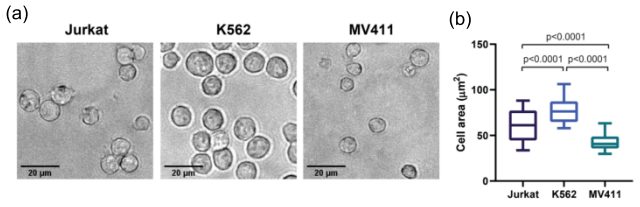

Fig. 3. (a) Images of the three leukemia cell lines in culture (Jurkat, K562, and MV-411 cells). (b) Comparison of three leukemia cell areas.

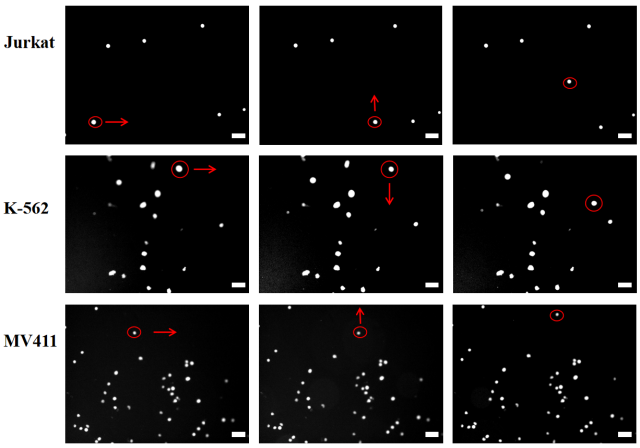

Fig. 4. Manipulation of three leukemia cells by following the designed motion paths (scale bar—100 μm).

performance and acoustic intensity to trap cell for manipulation. Fig. 4 shows the fluorescent images of Calcein AM stained live leukemia cells, showing the consecutive images of displacement of leukemia cells, which illustrates that the fabricated transducer was able to trap and manipulate cells. Cells could be constantly manipulated when their motion was followed by the designated movement of the transducer (see the supplementary videos 1, 2, and 3). In Fig. 4, cells were trapped from an arbitrary point first, and the arrows illustrated the designated moving direction of the transducer by stage controller while cells followed the same moving trails. Afterward, the cells were shifted by a designated motion path. It implied that applying developed acoustic tweezer has a great potential in manipulating or trapping cells, such as stem cells in the future, which brings more therapeutic feasibility for cell transplant and therapy.

B. Quantitative Analysis for Deformation of Trapped Cells (Jurkat, K562, and MV-411)

To evaluate the effectiveness of the acoustic tweezer system, the relative deformability of acoustically trapped and manipulated Jurkat, K562, and MV-411 cells were quantitatively measured and analyzed under acoustic peak pressure from 0.12 to 0.54 MPa. In Fig. 5, the morphological changes of manipulated cells at different acoustic pressures were shown and scrutinized. As the increasing input voltage led to the acoustic pressure increase, the areas of the cells were expanded. The relative deformability of the cell can be defined

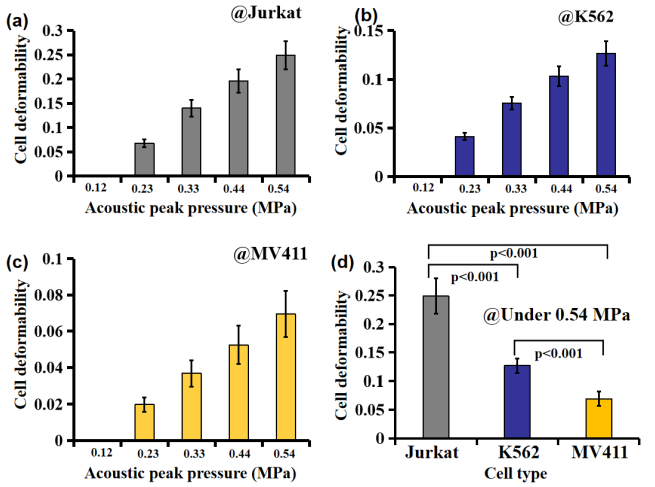

Fig. 5. (a) Mean cell deformability of Jurkat cells under acoustic peak pressure from 0.12 to 0.54 MPa ($n = 12$). (b) Mean cell deformability of K562 cells under acoustic peak pressure from 0.12 to 0.54 MPa ($n = 12$). (c) Mean cell deformability of MV-411 cells under acoustic peak pressure from 0.12 to 0.54 MPa ($n = 12$). (d) Mean cell deformability comparison of three leukemia cells under acoustic peak pressure of 0.54 MPa ($n = 12$).

as follows [41]:

$$\text{Deformability}(D) = \frac{\text{Area}_2 - \text{Area}_1}{\text{Area}_1} \tag{1}$$

wherein Area_1 represents the area of the trapped cell under initial acoustic peak pressure of 0.12 MPa, and Area_2 is the area of the trapped cell under different increased acoustic peak pressures. In Fig. 5(a)–(c), the relative deformability of the Jurkat, K562, and MV-411 cells under each acoustic peak pressure was quantitatively measured and calculated to investigate discrimination in mechanical properties of different leukemia cells. Different inputs from the signal generator can drive the high-frequency ultrasound transducer to transmit different single ultrasound beams. The mean deformabilities of Jurkat cells were determined approximately as 0.067–0.248 at acoustic peak pressures of 0.12–0.54 MPa, separately. For K562 cell, the mean deformabilities were calculated approximately to be 0.04–0.126 from 0.12 to 0.54 MPa, and the mean deformabilities of MV-411 cells were approximately analyzed as 0.019–0.069 at acoustic peak pressures of 0.12–0.54 MPa, respectively (Table I). In addition, we compared cell deformations under 0.54 MPa because this case shows the largest difference in deformability among the cells [Fig. 5(d)]. The results showed that Jurkat cells have been more relatively deformable than the other two cells, and the MV-411, which has the smallest relative deformability, exhibited less mechanosensitivity. Moreover, we can successfully distinguish each different type of leukemia cell line by characterizing their relative deformability without any direct contact and fluorescent dye.

C. Cell Viability Evaluation

To examine whether the acoustic stimulation is nondestructive to cells, the viability results of three cells were evaluated

TABLE I
AVERAGE OF DEFORMABILITY(D) DUE TO VARIOUS INPUTS (JURKAT, K562, AND MV-411)

Cases	0.12 MPa	0.23 MPa	0.33 MPa	0.44 MPa	0.54 MPa
Jurkat	0	0.067 ±0.008	0.139 ±0.017	0.196 ±0.024	0.248 ±0.029
K562	0	0.040 ±0.004	0.754 ±0.006	0.1033 ±0.010	0.126 ±0.012
MV411	0	0.019 ±0.004	0.036 ±0.007	0.052 ±0.010	*0.069* ±0.012

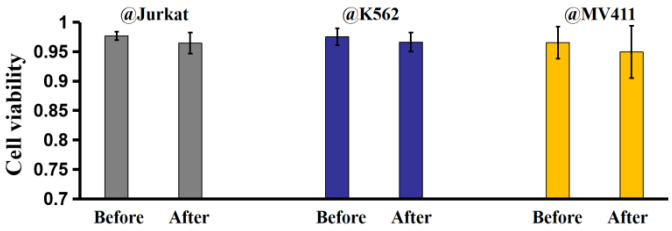

Fig. 6. Comparison of viabilities of Jurkat, K562, and MV-411 cells before cell trapping and after cell deformation ($n = 12$ for each cell).

TABLE II
QUANTITATIVE ANALYSIS OF VIABILITY OF EACH CELL BEFORE CELL TRAPPING AND AFTER CELL DEFORMATION (JURKAT, K562, AND MV-411)

Cases	Before	After	p-value
Jurkat	0.976 ±0.007	0.964 ±0.017	0.0226
K562	0.975 ±0.014	0.966 ±0.016	0.0583
MV411	0.965 ±0.027	0.949 ±0.044	0.156

before cell trapping and after cell deformation under 0.54 MPa for 25 min as the harshest condition among experiments. In Fig. 6, compared to the mean viability of each cell before trapping, the viability of each cell after cell deformation has been slightly decreased. The viability results for Jurkat, K562, and MV-411 cells before cell trapping were measured as 0.976 (standard deviation: ±0.007), 0.975 (standard deviation: ±0.014), and 0.965 (standard deviation: ±0.027), respectively, and the that of each cell after deformation were tested as 0.964 (standard deviation: ±0.017), 0.966 (standard deviation: ±0.016), and 0.949 (standard deviation: ±0.044), respectively. Moreover, the p-values of Jurkat, K562, and MV-411 were calculated as 0.0226, 0.0583, and 0.156, separately, which are all exceeding 0.01, showing that ultrasound beam did not significantly affect cell functions during cell deformation and cell trapping tests (Table II). From these results, our proposed system is allowed to distinguish the type of leukemia cells without the critical damage to the cell.

IV. DISCUSSION

From the various studies, mechanosensitivity could be correlated with increased cytoskeletal forces [58]. Cell stiffness or deformability is governed by the cellular components and has been correlated with cell motility [59]. In particular, migratory cells with higher motility have been characterized by both a softer nucleus and cortex actin network [60], [61]. Comparing the relative deformability trends of measured cells under different acoustic peak pressures, we showed that Jurkat cells have larger relative deformability under each acoustic peak pressure. Especially under the acoustic peak pressure of 0.54 MPa, the Jurkat cell has higher relative deformability of 0.248. It implied that increasing acoustic pressure by increasing input voltage is able to cause area change of trapped and manipulated leukemia cells, and Jurkat cells demonstrated better mechanical properties, which fitted well with the results characterized in the previous literature that Jurkat cells were softer [22], [58]. Moreover, after exposure to chemotherapy, acute lymphoblastic cell lines (HL-60 and Jurkat) possessed increased stiffness [62]. A study on stiffness/deformability of lymphocytes in chronic lymphocytic leukemia (CLL) patients measured by AFM showed decreased stiffness compared to cells from healthy donors [63]. Another study investigated the relationship between cell cycle (G0 versus G1) and stiffness of cells in CML patients; however, it did not show a consistent trend due to high variations between patients [64]. In this study, the less deformable cells showed less cell mechanical sensitivity under the same acoustic peak pressure. Based on the definition of Young's modulus, stress and strain are needed to be measured. In the acoustic tweezer system, the accurate value of acoustic radiation force on the cells is hard to be calibrated; hence, the stress is unknown but kept as a constant value as the same acoustic pressure was applied during the deformation test. Thus, the strain could directly reflect the relative value of Young's modulus. To allow us to compare with the existing methods (e.g., AFM and optical tweezer), in the future, we will explore and investigate the relative axial strain to study Young's modulus by utilizing our developed acoustic tweezer system, which will allow us to further study the relationship between cell deformability and cell stiffness, and we will also focus on using our developed acoustic tweezer system to apply chemical drugs in the leukemia cells to see the therapeutic effect. To date, the relationship between the pathology of different leukemia types and cell stiffness remains a matter of debate. Thus, our developed acoustic tweezer technique will inspire more studies and investigations in actin cytoskeletal dynamics and the underlying mechanism of signaling activation in adaptive immune response in the body, which will have a good influence on the study of human immune response and vaccine development.

V. CONCLUSION

In conclusion, a 50-MHz high-frequency LNO ultrasound transducer was fabricated and applied in an acoustic tweezer system developed in-house, which was capable of trapping and manipulating the selected leukemia cells, including Jurkat, K562, and MV-411 cells. Moreover, with increasing the acoustic pressure, the manipulated leukemia cells were stretched and deformed, and the relative deformability of the single cell was analyzed to characterize the cell mechanical property. The Jurkat cell achieved higher deformability.

It shows that the high-frequency acoustic tweezer system has quite the potential to replace other biophysical tools, such as AFM or optical tweezers, to quantify cell mechanics without contacting targeted cells. Significantly, the deformability comparison of selected leukemia cells also brings more possibilities to study the cytoskeletal dynamics and potential mechanisms of signaling activation in the immune system. Meanwhile, it also inspires further studies on employing the ultrasound array in the application of the high-frequency ultrasound beam to manipulate different cells and characterize the elasticity and Young's modulus of cells in the future. From this outcome, our proposed system can be the foundation for providing next-generated cancer treatment by characterizing the mechanical properties of different types of leukemia cells.

REFERENCES

[1] B. Plusa and A.-K. Hadjantonakis, "Mechanics drives cell differentiation," *Nature*, vol. 536, no. 7616, pp. 281–282, Aug. 2016.

[2] U. F. Greber, "How cells tune viral mechanics—Insights from biophysical measurements of influenza virus," *Biophys. J.*, vol. 106, no. 11, pp. 2317–2321, 2014.

[3] T. M. J. Evers, L. J. Holt, S. Alberti, and A. Mashaghi, "Reciprocal regulation of cellular mechanics and metabolism," *Nature Metabolism*, vol. 3, no. 4, pp. 456–468, Apr. 2021.

[4] Z. Liu *et al.*, "Cancer cells display increased migration and deformability in pace with metastatic progression," *FASEB J.*, vol. 34, no. 7, pp. 9307–9315, Jul. 2020.

[5] S. Byun *et al.*, "Characterizing deformability and surface friction of cancer cells," *Proc. Nat. Acad. Sci. USA*, vol. 110, no. 19, pp. 7580–7585, 2013.

[6] G. Calibasi Kocal *et al.*, "Dynamic microenvironment induces phenotypic plasticity of esophageal cancer cells under flow," *Sci. Rep.*, vol. 6, no. 1, pp. 1–11, Dec. 2016.

[7] W. Xu, R. Mezencev, B. Kim, L. Wang, J. McDonald, and T. Sulchek, "Cell stiffness is a biomarker of the metastatic potential of ovarian cancer cells," *PLoS ONE*, vol. 7, no. 10, Oct. 2012, Art. no. e46609.

[8] H.-C. Liu *et al.*, "Characterizing deformability of drug resistant patient-derived acute lymphoblastic leukemia (ALL) cells using acoustic tweezers," *Sci. Rep.*, vol. 8, no. 1, pp. 1–10, Dec. 2018.

[9] Y. Tan, T.-K. Fung, H. Wan, K. Wang, A. Y. H. Leung, and D. Sun, "Biophysical characterization of hematopoietic cells from normal and leukemic sources with distinct primitiveness," *Appl. Phys. Lett.*, vol. 99, no. 8, Aug. 2011, Art. no. 083702.

[10] R. S. Mehta, B. Randolph, M. Daher, and K. Rezvani, "NK cell therapy for hematologic malignancies," *Int. J. Hematology*, vol. 107, no. 3, pp. 262–270, Mar. 2018.

[11] M.-T. Wang *et al.*, "Blockade of leukemia inhibitory factor as a therapeutic approach to KRAS driven pancreatic cancer," *Nature Commun.*, vol. 10, no. 1, pp. 1–10, Dec. 2019.

[12] K. McLean *et al.*, "Leukemia inhibitory factor functions in parallel with interleukin-6 to promote ovarian cancer growth," *Oncogene*, vol. 38, no. 9, pp. 1576–1584, Feb. 2019.

[13] C. Zhang, J. Liu, J. Wang, W. Hu, and Z. Feng, "The emerging role of leukemia inhibitory factor in cancer and therapy," *Pharmacol. Therapeutics*, vol. 221, May 2021, Art. no. 107754.

[14] Y. Jia, W.-J. Chng, and J. Zhou, "Super-enhancers: Critical roles and therapeutic targets in hematologic malignancies," *J. Hematol. Oncol.*, vol. 12, no. 1, pp. 1–17, Dec. 2019.

[15] J. C. Reed and M. Pellecchia, "Apoptosis-based therapies for hematologic malignancies," *Blood*, vol. 106, no. 2, pp. 408–418, Jul. 2005.

[16] O. Ngalamika, Y. Zhang, H. Yin, M. Zhao, M. E. Gershwin, and Q. Lu, "Epigenetics, autoimmunity and hematologic malignancies: A comprehensive review," *J. Autoimmunity*, vol. 39, no. 4, pp. 451–465, Dec. 2012.

[17] C.-H. Pui and W. E. Evans, "Treatment of acute lymphoblastic leukemia," *New England J. Med.*, vol. 354, no. 2, pp. 166–178, 2006.

[18] J. Saultz and R. Garzon, "Acute myeloid leukemia: A concise review," *J. Clin. Med.*, vol. 5, no. 3, p. 33, Mar. 2016.

[19] J. E. Cortes, M. Talpaz, and H. Kantarjian, "Chronic myelogenous leukemia: A review," *Amer. J. Med.*, vol. 100, no. 5, pp. 555–570, 1996.

[20] A. Redaelli, J. M. Stephens, B. L. Laskin, C. L. Pashos, and M. F. Botteman, "The burden and outcomes associated with four leukemias: AML, ALL, CLL and CML," *Expert Rev. Anticancer Therapy*, vol. 3, no. 3, pp. 311–329, Jun. 2003.

[21] T. Somer and H. J. Meiselman, "Disorders of blood viscosity," *Ann. Med.*, vol. 25, no. 1, pp. 31–39, Jan. 1993.

[22] M. J. Rosenbluth, W. A. Lam, and D. A. Fletcher, "Force microscopy of nonadherent cells: A comparison of leukemia cell deformability," *Biophys. J.*, vol. 90, no. 8, pp. 2994–3003, Apr. 2006.

[23] L. Hu *et al.*, "Decreased cell stiffness enhances leukemia development and progression," *Leukemia*, vol. 34, no. 9, pp. 2493–2497, Sep. 2020.

[24] F. Ni *et al.*, "Ptpn21 controls hematopoietic stem cell homeostasis and biomechanics," *Cell Stem Cell*, vol. 24, no. 4, pp. 608–620, 2019.

[25] B. G. Hosu, K. Jakab, P. Bánki, F. I. Tóth, and G. Forgacs, "Magnetic tweezers for intracellular applications," *Rev. Sci. Instrum.*, vol. 74, no. 9, pp. 4158–4163, 2003.

[26] D. Kilinc and G. U. Lee, "Advances in magnetic tweezers for single molecule and cell biophysics," *Integrative Biol.*, vol. 6, no. 1, pp. 27–34, 2014.

[27] M. Tanase, N. Biais, and M. Sheetz, "Magnetic tweezers in cell biology," *Methods Cell Biol.*, vol. 83, pp. 473–493, Jan. 2007.

[28] X. Wang *et al.*, "Intracellular manipulation and measurement with multipole magnetic tweezers," *Sci. Robot.*, vol. 4, no. 28, Mar. 2019.

[29] C. Arbore, L. Perego, M. Sergides, and M. Capitanio, "Probing force in living cells with optical tweezers: From single-molecule mechanics to cell mechanotransduction," *Biophys. Rev.*, vol. 11, no. 5, pp. 765–782, Oct. 2019.

[30] R. Zhu, T. Avsievich, A. Popov, and I. Meglinski, "Optical tweezers in studies of red blood cells," *Cells*, vol. 9, no. 3, p. 545, Feb. 2020.

[31] P. Polimeno *et al.*, "Optical tweezers and their applications," *J. Quant. Spectrosc. Radiat. Transf.*, vol. 218, pp. 131–150, Oct. 2018.

[32] C. Bustamante, L. Alexander, K. Maciuba, and C. M. Kaiser, "Single-molecule studies of protein folding with optical tweezers," *Annu. Rev. Biochem.*, vol. 89, no. 1, pp. 443–470, Jun. 2020.

[33] M. Li, N. Xi, Y. Wang, and L. Liu, "Advances in atomic force microscopy for single-cell analysis," *Nano Res.*, vol. 12, no. 4, pp. 703–718, Apr. 2019.

[34] Y. F. Dufrêne *et al.*, "Imaging modes of atomic force microscopy for application in molecular and cell biology," *Nature Nanotechnol.*, vol. 12, no. 4, pp. 295–307, 2017.

[35] M. Krieg *et al.*, "Atomic force microscopy-based mechanobiology," *Nature Rev. Phys.*, vol. 1, no. 1, pp. 41–57, 2019.

[36] J.-S. Huang and Y.-T. Yang, "Origin and future of plasmonic optical tweezers," *Nanomaterials*, vol. 5, no. 2, pp. 1048–1065, Jun. 2015.

[37] M. J. Lang and S. M. Block, "Resource letter: LBOT-1: Laser-based optical tweezers," *Amer. J. Phys.*, vol. 71, no. 3, pp. 201–215, Mar. 2003.

[38] I. Titushkin and M. Cho, "Distinct membrane mechanical properties of human mesenchymal stem cells determined using laser optical tweezers," *Biophys. J.*, vol. 90, no. 7, pp. 2582–2591, Apr. 2006.

[39] R. Agarwal and K. E. Duderstadt, "Multiplex flow magnetic tweezers reveal rare enzymatic events with single molecule precision," *Nature Commun.*, vol. 11, no. 1, pp. 1–10, Dec. 2020.

[40] W. I. Moghram, P. Singh, C. A. VandeLune, E. A. Sander, and J. C. Selby, "Integration of magnetic tweezers and traction force microscopy for the exploration of matrix rheology and keratinocyte mechanobiology: Model force- and displacement-controlled experiments," *AIP Adv.*, vol. 11, no. 4, 2021, Art. no. 045216.

[41] J. Y. Hwang *et al.*, "Cell deformation by single-beam acoustic trapping: A promising tool for measurements of cell mechanics," *Sci. Rep.*, vol. 6, no. 1, pp. 1–8, Jun. 2016.

[42] H. C. Liu *et al.*, "Integrin antibody decreases deformability of patient-derived pre-B acute lymphocytic leukemia cells as measured by high-frequency acoustic tweezers," *J. Ultrasound Med.*, vol. 39, no. 3, pp. 589–595, 2020.

[43] J. Y. Hwang, C. Lee, K. H. Lam, H. H. Kim, J. Lee, and K. K. Shung, "Cell membrane deformation induced by a fibronectin-coated polystyrene microbead in a 200-MHz acoustic trap," *IEEE Trans. Ultrason., Ferroelectr., Freq. Control*, vol. 61, no. 3, pp. 399–406, Mar. 2014.

[44] J. Y. Hwang *et al.*, "Acoustic tweezers for studying intracellular calcium signaling in SKBR-3 human breast cancer cells," *Ultrasonics*, vol. 63, pp. 94–101, Dec. 2015.

[45] X. Chen *et al.*, "Helical-Like 3D ultrathin piezoelectric element for complicated ultrasonic field," *Adv. Funct. Mater.*, vol. 29, no. 32, 2019, Art. no. 1902912.

[46] X. Chen *et al.*, "An adjusatable multi-scale single beam acoustic tweezers based on ultrahigh frequency ultrasonic transducer," *Biotechnol. Bioeng.*, vol. 114, no. 11, pp. 2637–2647, 2017.
[47] X. Chen *et al.*, "Acoustic levitation and manipulation by a high-frequency focused ring ultrasonic transducer," *Appl. Phys. Lett.*, vol. 114, no. 5, Feb. 2019, Art. no. 054103.
[48] K. H. Lam, Y. Li, Y. Li, H. G. Lim, Q. Zhou, and K. K. Shung, "Multifunctional single beam acoustic tweezer for non-invasive cell/organism manipulation and tissue imaging," *Sci. Rep.*, vol. 6, no. 1, pp. 1–7, Dec. 2016.
[49] H. G. Lim *et al.*, "Investigation of cell mechanics using single-beam acoustic tweezers as a versatile tool for the diagnosis and treatment of highly invasive breast cancer cell lines: An *in vitro* study," *Microsyst. Nanoeng.*, vol. 6, no. 1, pp. 1–12, Dec. 2020.
[50] H. G. Lim, O.-J. Lee, K. K. Shung, J.-T. Kim, and H. H. Kim, "Classification of breast cancer cells using the integration of high-frequency single-beam acoustic tweezers and convolutional neural networks," *Cancers*, vol. 12, no. 5, p. 1212, May 2020.
[51] S. Youn *et al.*, "Acoustic trapping technique for studying calcium response of a suspended breast cancer cell: Determination of its invasion potentials," *IEEE Trans. Ultrason., Ferroelectr., Freq. Control*, vol. 66, no. 4, pp. 737–746, Apr. 2019.
[52] S. Youn, K. Lee, J. Son, I.-H. Yang, and J. Y. Hwang, "Fully-automatic deep learning-based analysis for determination of the invasiveness of breast cancer cells in an acoustic trap," *Biomed. Opt. Exp.*, vol. 11, no. 6, pp. 2976–2995, 2020.
[53] J. A. Jensen and N. B. Svendsen, "Calculation of pressure fields from arbitrarily shaped, apodized, and excited ultrasound transducers," *IEEE Trans. Ultrason., Ferroelectr., Freq. Control*, vol. 39, no. 2, pp. 262–267, Mar. 1992.
[54] J. A. Jensen, "Field: A program for simulating ultrasound systems," in *Proc. 10th NORDICBALTIC Conf. Biomed. Imag.*, 1996, vol. 4, no. 1, pp. 351–353.
[55] D. Baresch, J.-L. Thomas, and R. Marchiano, "Observation of a single-beam gradient force acoustical trap for elastic particles: Acoustical tweezers," *Phys. Rev. Lett.*, vol. 116, no. 2, Jan. 2016, Art. no. 024301.
[56] J. Lee, K. Ha, and K. K. Shung, "A theoretical study of the feasibility of acoustical tweezers: Ray acoustics approach," *J. Acoust. Soc. Amer.*, vol. 117, no. 5, pp. 3273–3280, May 2005.
[57] P. Mishra, M. Hill, and P. Glynne-Jones, "Deformation of red blood cells using acoustic radiation forces," *Biomicrofluidics*, vol. 8, no. 3, May 2014, Art. no. 034109.
[58] K. L. Hui, L. Balagopalan, L. E. Samelson, and A. Upadhyaya, "Cytoskeletal forces during signaling activation in jurkat T-cells," *Mol. Biol. Cell*, vol. 26, no. 4, pp. 685–695, Feb. 2015.
[59] Q. Luo, D. Kuang, B. Zhang, and G. Song, "Cell stiffness determined by atomic force microscopy and its correlation with cell motility," *Biochim. et Biophys. Acta (BBA)-Gen. Subjects*, vol. 1860, no. 9, pp. 1953–1960, Sep. 2016.
[60] P. Friedl, K. Wolf, and J. Lammerding, "Nuclear mechanics during cell migration," *Current Opinion Cell Biol.*, vol. 23, no. 1, pp. 55–64, Feb. 2011.
[61] S. Suetsugu and T. Takenawa, "Regulation of cortical actin networks in cell migration," *Int. Rev. Cytol.*, vol. 229, pp. 245–286, 2003.
[62] W. A. Lam, M. J. Rosenbluth, and D. A. Fletcher, "Chemotherapy exposure increases leukemia cell stiffness," *Blood*, vol. 109, no. 8, pp. 3505–3508, Apr. 2007.
[63] Y. Zheng, J. Wen, J. Nguyen, M. A. Cachia, C. Wang, and Y. Sun, "Decreased deformability of lymphocytes in chronic lymphocytic leukemia," *Sci. Rep.*, vol. 5, no. 1, pp. 1–5, Jul. 2015.
[64] N. V. Guz, S. J. Patel, M. E. Dokukin, B. Clarkson, and I. Sokolov, "Biophysical differences between chronic myelogenous leukemic quiescent and proliferating stem/progenitor cells," *Nanomed., Nanotechnol., Biol. Med.*, vol. 12, no. 8, pp. 2429–2437, Nov. 2016.

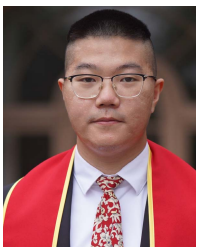

Yushun Zeng (Member, IEEE) received the B.Eng. degree in bioengineering from Nanjing Tech University, Nanjing, China, in 2019, and the M.S. degree in biomedical engineering from the University of Southern California, Los Angeles, CA, USA, in 2021, where he is currently pursuing the Ph.D. degree with the Department of Biomedical Engineering.

His research interests mainly focus on the fabrication of high-frequency ultrasound transducer/array, 3-D-printed ultrasonic device, and development of high-frequency acoustic tweezer.

Jia Hao received the bachelor's degree in materials science and engineering from the University of Science and Technology Beijing, Beijing, China, in 2015, and the master's degree in materials science and engineering from Cornell University, Ithaca, NY, USA, in 2017. She is currently pursuing the Ph.D. degree in biomedical engineering with Dr. Keyue Shen's Laboratory, University of Southern California, Los Angeles, CA, USA.

She is currently working with Dr. Keyue Shen's Laboratory, University of Southern California. Her research focuses on understanding membrane bound regulation of hematopoietic stem cells using *in vitro* models.

Junhang Zhang (Member, IEEE) received the M.S. degree in biomedical engineering from the University of Southern California, Los Angeles, CA, USA, in 2020, where he is currently pursuing the Ph.D. degree with the Department of Biomedical Engineering.

His current interests include the development of high-frequency transducer and ultrasonic elastography.

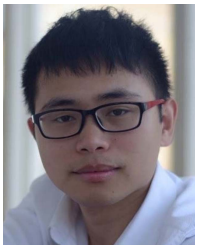

Laiming Jiang received the Ph.D. degree in materials physics and chemistry from the Department of Materials Science and Engineering, Sichuan University, Chengdu, China, in 2019.

He is currently a Postdoctoral Scholar with the Keck School of Medicine, University of Southern California (USC), Los Angeles, CA, USA. His research interests include lead-free piezoelectric materials, ultrasound transducers/arrays, energy harvesting, multiscale and multimaterial 3-D printing, and bio-implantable devices.

Sangyeon Youn received the B.S. degree in biomedical engineering and chemical engineering from Chonbuk National University, Jeonju, South Korea, in 2016, and the M.S. degree from the Department of Information and Communication Engineering, Daegu Gyeongbuk Institute of Science and Technology, Daegu, South Korea, in 2018, where he is currently pursuing the Ph.D. degree.

He is currently a Visiting Scholar with the Department of Biomedical Engineering, University of Southern California, Los Angeles, CA, USA. His current research interests include the multimodal imaging system based on high-frequency ultrasound, fabrication of high-frequency ultrasound transducer, and acoustic trapping technique by using high-frequency single element transducer.

Gengxi Lu (Member, IEEE) received the bachelor's degree in physics from Nanjing University, Nanjing, China, in 2017. He is currently pursuing the Ph.D. degree with the Department of Biomedical Engineering, University of Southern California, Los Angeles, CA, USA.

His research interests include the ultrasound neuromodulation, ultrasound imaging and elastography, 3-D printing, and the development of ultrasound transducers.

Dongliang Yan received the B.S. degree in ecology from Shandong Agricultural University, Taian, China, in 2020. He is currently pursuing the degree with the Department of Biomedical Engineering, University of Southern California, Los Angeles, CA, USA.

His research focus includes the ultrasound transducer design and fabrication and development of the ultrasound tweezer.

Haochen Kang (Graduate Student Member, IEEE) received the B.Eng. degree in electrical engineering from the Huazhong University of Science and Technology, Wuhan, China, in 2015, and the M.S. degree in electrical engineering from the University of Southern California, Los Angeles, CA, USA, in 2017, where he is currently pursuing the Ph.D. degree in biomedical engineering.

His research is focused on the design and application of 2-D ultrasound systems.

Yizhe Sun (Member, IEEE) received the B.S. degree in aircraft engineering and design from the Nanjing University of Aeronautics and Astronautics, Nanjing, China, in 2017. He is currently pursuing the Ph.D. degree with the Ultrasound Transducer Research Center, University of Southern California (USC), Los Angeles, CA, USA.

From January 2018 to July 2018, he worked as a Research Assistant with The Hong Kong University of Science and Technology, Hong Kong. He is currently the Laboratory Manager with the Ultrasound Transducer Research Center, USC, working to develop the ultrasound array and single element transducers. He is proficient in mechanical engineering and microelectromechanical systems (MEMS). He plans to continue his work in academia, which include the design and fabrication of high-frequency ultrasonic transducers and arrays.

K. Kirk Shung (Life Fellow, IEEE) received the B.S. degree in electrical engineering (EE) from National Cheng Kung University, Tainan, Taiwan, in 1968, and the Ph.D. degree in EE from the University of Washington, Seattle, WA, USA, in 1975.

He was the Dean and a Professor in biomedical engineering with the Viterbi School of Engineering, University of Southern California (USC), Los Angeles, CA, USA, from 2013 to 2018, where he became the Dwight C. and Hildagarde E. Baum Chair of biomedical engineering in 2018. He has been a Professor of biomedical engineering with USC, since 2002. He has published more than 500 articles and book chapters. He has written two textbooks. His research interests include ultrasonic transducers, high-frequency ultrasonic imaging, and applications in cellular bioengineering.

Dr. Shung is a fellow of the American Institute of Ultrasound in Medicine and a founding fellow of the American Institute of Medical and Biological Engineering. He was a recipient of the IEEE Engineering in Medicine and Biology Society Early Career Award in 1985, the Holmes Pioneer Award in Basic Science from the American Institute of Ultrasound in Medicine in 2010, the Academic Career Achievement Award from the IEEE Engineering in Medicine and Biology Society in 2011, and the IEEE Biomedical Engineering Award in 2016. He was a coauthor of an article that received the Best Paper Award for the IEEE TRANSACTIONS ON ULTRASONICS, FERROELECTRICS AND FREQUENCY CONTROL (UFFC) in 2000. He was elected as an Outstanding Alumnus of National Cheng Kung University in 2001. He was selected as a Distinguished Lecturer of the IEEE UFFC Society from 2002 to 2003. He is an Associate Editor of the IEEE TRANSACTIONS ON BIOMEDICAL ENGINEERING and *Medical Physics.*

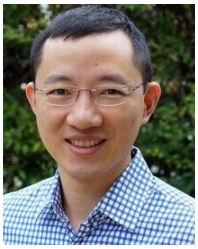

Keyue Shen received the B.Eng. degree (*summa cum laude*) in mechanical engineering and the M.Sc. degree in biophysics from Tsinghua University, Beijing, China, in 2001 and 2004, respectively, and the Ph.D. degree (Hons.) in biomedical engineering from the Department of Biomedical Engineering, Columbia University, New York City, NY, USA, in 2010.

He held a postdoctoral training with the Center for Engineering in Medicine, Harvard Medical School, Massachusetts General Hospital, Boston, MA, USA, where he won the MGH Fund for Medical Discovery Award. He joined the Department of Biomedical Engineering, University of Southern California (USC), Los Angeles, CA, USA, in January 2015. His research is also supported by the Phi Beta Psi Trust Fund. His research interests are in developing *in vitro* microengineered models of cell microenvironments in immune system, cancer, and stem cell niches, for applications in immune and cancer therapeutics, as well as cell/tissue regeneration.

Dr. Shen has since received the Marni Levine Memorial Research Development Award from STOP CANCER, the Trailblazer Award from National Institute of Biomedical Imaging and Bioengineering (NIBIB) at the National Institutes of Health (NIH), and the Rose Hills Research Fellowship from USC.

Qifa Zhou (Fellow, IEEE) received the Ph.D. degree from the Department of Electronic Materials and Engineering, Xi'an Jiaotong University, Xi'an, China, in 1993.

Before joining the University of Southern California (USC), Los Angeles, CA, USA, in 2002, he worked with the Department of Physics, Sun Yat-sen University, Guangzhou, China; the Department of Applied Physics, The Hong Kong Polytechnic University, Hong Kong; and the Materials Research Laboratory, Pennsylvania State University, State College, PA, USA. He is currently a Professor of biomedical engineering and ophthalmology with USC. He has authored or coauthored more than 200 peer-reviewed articles in journals including *Nature Medicine*, *Advanced Materials*, and *Progress in Materials Science*. His research focuses on the development of piezoelectric high-frequency ultrasonic transducers for biomedical ultrasound and photoacoustic imaging, including intravascular imaging, cancer imaging, and ophthalmic imaging. He is also actively exploring ultrasonic mediated therapeutic technology including trans-sclera drug delivery, as well as ultrasound for retinal and brain stimulation.

Dr. Zhou is a fellow of the International Society for Optics and Photonics (SPIE) and the American Institute for Medical and Biological Engineering (AIMBE) and a member of the Technical Program Committee of the IEEE International Ultrasonics Symposium. He is an Associate Editor of the IEEE TRANSACTIONS ON ULTRASONICS, FERROELECTRICS, AND FREQUENCY CONTROL.